Angiotensin II–induced cardiovascular load regulates cardiac remodeling and related gene expression in late-gestation fetal sheep

Andrew W. Norris[1], Timothy M. Bahr[1], Thomas D. Scholz[1], Emily S. Peterson[1], Ken A. Volk[1] and Jeffrey L. Segar[1]

BACKGROUND: Angiotensin II (ANG II) stimulates fetal heart growth, although little is known regarding changes in cardiomyocyte endowment or the molecular pathways mediating the response. We measured cardiomyocyte proliferation and morphology in ANG II–treated fetal sheep and assessed transcriptional pathway responses in ANG II and losartan (an ANG II type 1 receptor antagonist) treated fetuses.

METHODS: In twin-gestation pregnant sheep, one fetus received ANG II (50 µg/kg/min i.v.) or losartan (20 mg/kg/d i.v.) for 7 d; noninstrumented twins served as controls.

RESULTS: ANG II produced increases in heart mass, cardiomyocyte area (left ventricle (LV) and right ventricle mononucleated and LV binucleated cells), and the percentage of Ki-67–positive mononucleated cells in the LV (all $P < 0.05$). ANG II and losartan produced generally opposing changes in gene expression, affecting an estimated 55% of the represented transcriptome. The most prominent significantly affected biological pathways included those involved in cytoskeletal remodeling and cell cycle activity.

CONCLUSION: ANG II produces an increase in fetal cardiac mass via cardiomyocyte hypertrophy and likely hyperplasia, involving transcriptional responses in cytoskeletal remodeling and cell cycle pathways.

Remodeling responses to biomechanical and neurohumoral stimuli have been extensively documented in the fetal, neonatal, and adult heart (1,2). Each of these developmental stages poses a different functional environment for the heart, resulting in distinct morphologic, genomic, and proteomic responses. For example, only the fetal heart is composed of a substantial number of mononucleated rather than multinucleated cardiomyocytes (3). Underlying developmental differences accompanied by respective diversity in protein expression likely result in differential cardiac adaptive responses to growth-promoting stimuli.

Angiotensin II (ANG II) exerts multiple direct and indirect effects on the heart. ANG II stimulates type 1 (AT_1) and type 2 (AT_2) receptors on cardiomyocytes and vascular smooth muscle, resulting in altered cardiac structure and function from direct myocardial effects as well as from increased afterload. Direct effects of ANG II on cardiomyocytes have been described for fetal, neonatal, and adult tissues (reviewed in Schlüter and Wenzel (4)). The majority of these studies have been performed in isolated cardiomyocytes, which may or may not reflect what occurs *in vivo*. We previously demonstrated that elevated ANG II levels result in an increase in fetal sheep left ventricular mass (5). However, whether this *in vivo* effect was related to cardiomyocyte hyperplasia, hypertrophy, or both, as occurs with increased afterload produced by fetal pulmonary artery banding or chronic plasma infusion, is not known (3,5). Based on these previous studies, we hypothesized that chronic infusion of ANG II increases fetal cardiac mass through cardiomyocyte hyperplasia and hypertrophy. We additionally sought to investigate potential mechanisms regulating cardiomyocyte fate in fetuses exposed to ANG II by determining the levels of terminal proteins of the mitogen-activated protein kinase (MAPK) and phosphatidylinositol 3-kinase/protein kinase B (AKT) signaling pathways. We further undertook a transcriptome-wide discovery approach to provide information on the biological pathways regulating myocardial responses in fetuses treated with ANG II and losartan, an AT_1 receptor antagonist. The effects of reduced systolic load on cardiomyocyte morphometry were not examined in the losartan-treated animals as this strategy has previously been studied using enalaprilat (6).

RESULTS

Thirty fetuses from 15 pregnant ewes were studied, with 10 fetuses receiving ANG II, 5 fetuses receiving losartan, and 15 fetuses serving as twin-matched controls. In the first group of fetuses, infusion of ANG II produced an increase in fetal mean arterial pressure from 44 ± 2 mm Hg on day 0 to 58 ± 3 mm Hg on day 6 (**Table 1**; $P < 0.05$). No significant changes in fetal heart rate or arterial blood gas values were identified. For the second group of study, which provided the opportunity to determine ventricular mass and isolation of protein and RNA, ANG II produced a similar increase in

The first two authors contributed equally to this work.

[1]Department of Pediatrics, University of Iowa Carver College of Medicine, Iowa City, Iowa. Correspondence: Jeffrey L. Segar (jeffrey-segar@uiowa.edu)

Received 5 June 2013; accepted 19 December 2013; advance online publication 9 April 2014. doi:10.1038/pr.2014.37

fetal mean arterial pressure from 42 ± 3 mm Hg on day 0 to 60 ± 2 mm Hg on day 6 (Table 1; $P < 0.05$). Administration of losartan resulted in a decrease in fetal mean blood pressure from 43 ± 3 mm Hg on day 0 to 28 ± 3 mm Hg on day 6 (Table 1; $P < 0.05$). No statistical differences in fetal heart rate were observed over this period. Arterial blood gas values, including pH, PcO_2, and PO_2 did not change over time in the ANG II–infused fetuses, whereas PO_2 decreased in the losartan-treated fetuses with PcO_2 and pH remaining unchanged (Table 1).

Fetal weight was similar among all groups of animals. The effects of altering arterial pressure by ANG II and losartan on the fetal heart mass are given in Table 1. Because one group of ANG II–infused fetuses ($n = 5$) and their matched controls were utilized for enzymatic cardiomyocyte dissociation, weights of individual heart components were not obtained.

Table 1. Somatic, hemodynamic, and arterial blood values in fetuses infused with angiotensin II or losartan

	Angiotensin II ($n = 5$)[a]	Control ($n = 10$)	Losartan ($n = 5$)	Angiotensin II ($n = 5$)
Sex	2m, 3f	6m, 4f	2m, 3f	3m, 2f
Age, day of gestation	131 ± 1	131 ± 1	131 ± 1	131 ± 1
MABP, mm Hg				
d0	44 ± 2	–	43 ± 3	42 ± 3
d6	58 ± 3	–	28 ± 3†	60 ± 2†
Heart rate, bpm				
d0	166 ± 9	–	159 ± 6	158 ± 8
d6	155 ± 6	–	154 ± 10	161 ± 10
pH				
d0	7.38 ± 0.11	–	7.36 ± 0.1	7.35 ± 0.00
d6	7.39 ± 0.01	–	7.34 ± 0.2	7.35 ± 0.00
PO_2, torr				
d0	17 ± 1	–	20 ± 1	19 ± 2
d6	18 ± 2	–	17 ± 1*	20 ± 2
PCO_2, torr				
d0	55 ± 3	–	52 ± 1	56 ± 2
d6	54 ± 2	–	56 ± 3	56 ± 2
Fetal weight (FW), kg	3.74 ± 0.15	3.80 ± 0.12	3.54 ± 0.12	3.36 ± 0.01
Heart, g	–	16.66 ± 1.03	14.00 ± 0.25	18.27 ± 0.90
Heart, g/kg FW	–	4.38 ± 0.21	3.96 ± 0.07	5.44 ± 0.27*
LV, g/kg FW	–	1.74 ± 0.06	1.69 ± 0.05	2.16 ± 0.11*
RV, g/kg FW	–	1.96 ± 0.15	1.60 ± 0.09	2.35 ± 0.20*

Heart weight represents sum of left ventricle (LV) and right ventricle (RV) free wall + septum weights.
d, day; f, female; m, male; MABP, mean arterial blood pressure; *n*, sample size for each group.
[a]Initial group of angiotensin II–infused fetuses utilized for isolated cardiomyocyte morphology. *$P < 0.05$ compared with control and losartan values. †$P < 0.05$ compared with d0 values.

For animals in the second group of study, left ventricle (LV), right ventricle (RV), septum, and total heart weight (LV + RV + septum), expressed per kg fetal body weight, were significantly greater in ANG II–treated fetuses as compared with control or losartan-treated animals. Cardiac weights following losartan treatment were not statistically different from controls.

ANG II–infused fetuses displayed significant increases in the area of LV mono- and binucleated cardiomyocytes and RV mononucleated cardiomyocytes (Figure 1) resulting from increases in cell width but not length (Figure 1). The percent binucleation (used as an index of terminal differentiation) of cardiomyocytes was not different between groups (Figure 2). Ki-67 staining, a marker of cell cycle activity, was significantly greater in the LV of ANG II–infused animals as compared with controls, whereas no difference was identified in the RV (Figure 2).

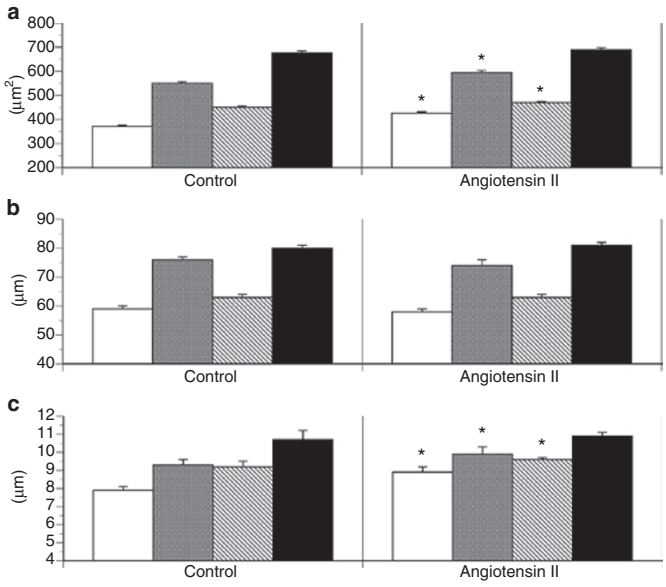

Figure 1. Effect of angiotensin II infusion on fetal ventricular cardiomyocyte (**a**) cell area, (**b**) cell length, and (**c**) cell width in left ventricle mononucleated cells (white bars); left ventricle binucleated cells (gray bars); right ventricle mononucleated cells (diagonal stripe bars); and right ventricle binucleated cells (black bars). Values are expressed as means ± SE. *$P < 0.05$ compared with control of similar cell type.

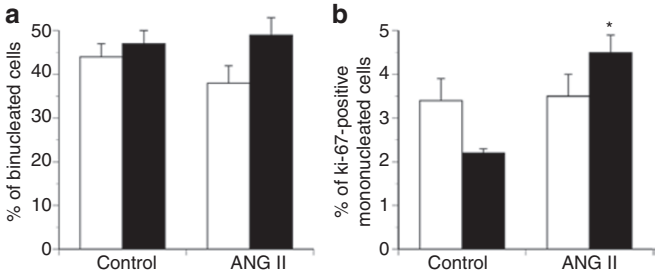

Figure 2. Effect of angiotensin II (ANG II) infusion on (**a**) fetal cardiomyocyte binucleation (maturation) and (**b**) Ki-67–positive immunostaining of mononucleated cells. White bars, right ventricle; black bars, left ventricle. Values expressed as means ± SE ($n = 5$ for each group). *$P < 0.05$ compared with control in similar ventricle.

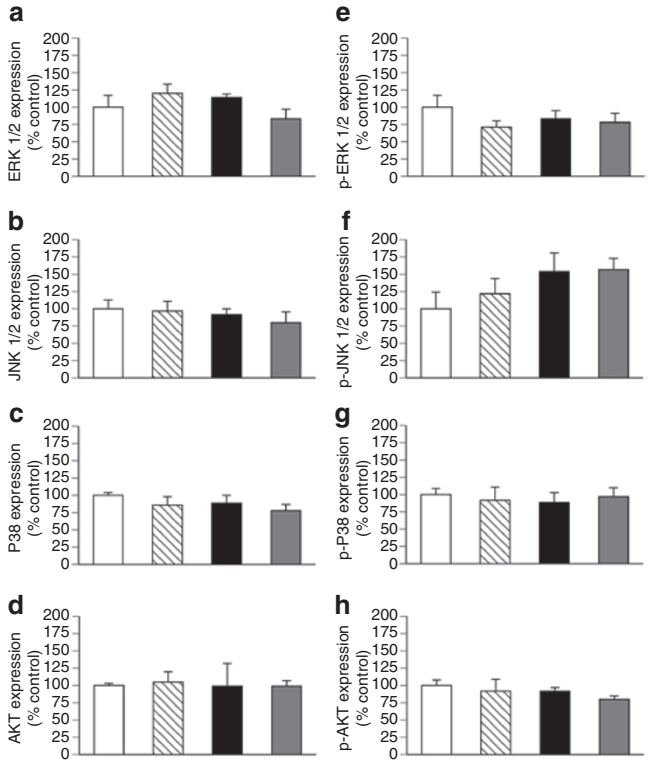

Figure 3. Effect of angiotensin II (ANG II) and losartan infusion on steady-state protein levels of (**a**–**d**) total and (**e**–**h**) activated mitogen-activated protein kinases (ERK 1/2, JNK 1/2, p38) and AKT 1 in fetal left ventricular myocardium. Control (twin of ANG II infused), white bar; ANG II infused, diagonal stripe bar; control (twin of losartan infused), black bar; losartan infused, gray bar. Values expressed as means ± SE ($n = 5$ for each group).

MAPK and AKT Signaling Pathways

ANG II and losartan had no effect on LV steady-state protein levels on total or the phosphorylated, active forms of ERK1/2, JNK, p38, or Akt1 as compared with controls (**Figure 3**).

Impact of Renin–Angiotensin Modulation on the Cardiac Transcriptome

Cardiac gene expression was assessed for four losartan-infused and four ANG II–infused fetuses and their control twins using the Agilent G4813A ovine microarray. The global impact of ANG II and losartan on gene expression segregated into separate groups (**Figure 4a**), suggesting that ANG II and losartan had distinct effects on gene expression. To further characterize the origins of this clustering pattern, we assessed principal expression components among those microarray features most impacted by ANG II and/or losartan. Interestingly, this demonstrated grouping of the ANG II vs. losartan hearts onto opposite sides of the principal component space (**Figure 4b**), with the control hearts located in the intervening space. By contrast, there was no such apparent grouping in control analyses in which the same procedures were performed on (i) those genes whose expression was most likely to not be impacted by losartan and ANG II and (ii) the dataset after randomization of group identities. Thus, among genes most affected by ANG II and/or losartan, the effects of these two interventions on gene expression tended to be in opposite directions, whereas the control hearts from the two groups tended to be similar to each other with intermediary expression.

ANOVA was used to identify the swath genes impacted by renin–angiotensin modulation by grouping samples as ANG

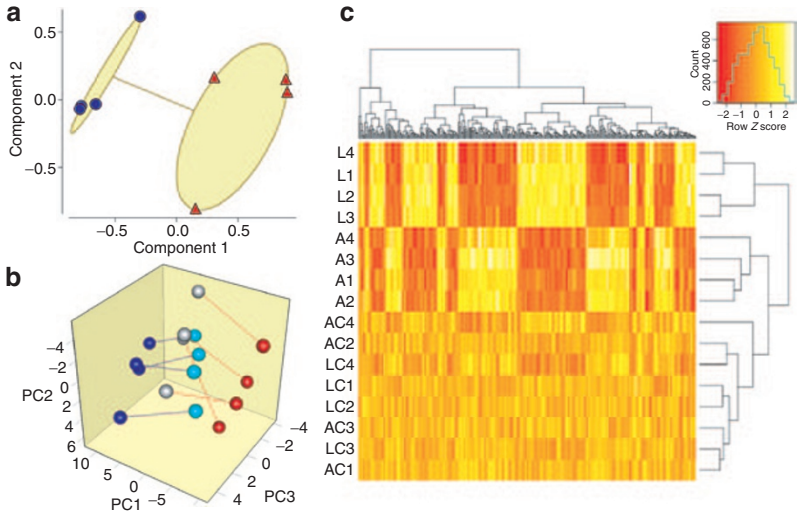

Figure 4. Impact of renin–angiotensin II (ANG II) modulation on the cardiac transcriptome. (**a**) Clustering analysis on all 15,208 microarray features. The effects of ANG II (red triangle) or losartan (blue circle) were isolated by subtracting control expression from expression in its corresponding intervention twin fetus. Components 1 and 2 explained 77% of the point variability. (**b**) Principal component analysis of genes whose expression was most likely affected by ANG II (red circle) vs. its twin (gray circle) and/or losartan (blue circle) vs. its control twin (aqua circle). Genes most likely affected were identified by $P < 0.0015$ by paired *t*-test for either intervention, which led to selection of 89 microarray features. Red lines indicate ANG II twinships; blue lines indicate losartan twinships. Axes represent principal components 1, 2, and 3 (PC1, PC2, and PC3, respectively), which accounted for 67% of the overall variance. (**c**) Hierarchical clustering of expression values of probes meeting stringent statistical significance defined by ANOVA based q value < 0.01. A total of 319 genes met this criteria and were clustered in both dimensions (columns = probes, samples = rows) using McQuitty's method and the maximum distance function in *R*. A, ANG II; AC, ANG II control; L, losartan; LC, losartan control; numbers refer to twinships (e.g., L3 and LC3 were twins). Inset: color key and histogram.

II, losartan, and control. Combining of control fetuses from both experimental interventions was appropriate because all eight control fetus expression features clustered together (Figure 4b) and received identical treatment. Although the ANOVA-based analysis estimated that 55% of the represented transcripts differed among the three groups, only one-fourth of these (14% of represented transcriptome) could be confidently identified at a positive false discovery rate (pFDR) of < 0.05. Hierarchical clustering was used to visualize the expression structure of the most significantly affected genes (pFDR < 0.01, 319 spots). Among these, genes upregulated by losartan tended to be downregulated by ANG II and vice versa (Figure 4c).

Of the 15,208 probe sequences on the sheep microarray, 11,087 were well annotated by interspecies homology, meeting the following criteria: (i) stringent homology demonstrating *E* value < 0.001, (ii) *blastn* accession mapped to a single entry, and (iii) identification of both gene symbol and organism. Of these, 8,638 were nonredundant. These annotations were based on closest homology to transcripts from *Bos taurus* (*N* = 5,953), *Ovis aries* (*N* = 717), *Sus scrofa* (*N* = 525), *Pan troglodytes* (*N* = 254), *Canis lupus familiaris* (*N* = 242), and other species. Homology to mammalian species accounted for 99.8% of the annotations. There were 1,520 well-annotated transcripts exhibiting differential expression among groups (pFDR < 0.05, **Supplementary Table S1** online). Of these, 675 were upregulated by ANG II and downregulated by losartan, 723 exhibited the opposing pattern, 69 were upregulated by both, and 53 were downregulated by both. The transcripts with the strongest statistical changes in expression in these four categories are detailed in **Supplementary Tables S2–S5** online.

Biological Pathways With Expression Impacted by Renin–Angiotensin Modulation

Of the 643 pathways in the MetaCore database, 243 demonstrated an overrepresentation of the genes significantly affected by ANG II and losartan by Fisher's exact test, controlling for FDR of 0.05. The top 25 pathways are shown in Table 2, and all statistically significant pathways are provided in **Supplementary Table S6** online.

Table 2. Top 25 scoring pathways altered by renin–angiotensin system modulation

Pathway	*q* Value
Cell cycle: role of APC in cell cycle regulation	2.97E-09
Development: TGF-β–dependent induction of epithelial-to-mesenchymal transition (EMT) via RhoA, PI3K, and ILK	7.50E-09
Cell cycle: the metaphase checkpoint	7.50E-09
Development: regulation of EMT	7.50E-09
Immune response: IL-6 signaling pathway	7.12E-08
Cytoskeleton remodeling: cytoskeleton remodeling	8.46E-08
Immune response: CD137 signaling in immune cell	2.33E-07
Cell cycle: initiation of mitosis	3.13E-07
Cytoskeleton remodeling: TGF, WNT, and cytoskeletal remodeling	3.70E-07
Cell cycle: chromosome condensation in prometaphase	5.40E-06
Development: TGF-β–dependent induction of EMT via MAPK	1.69E-05
Immune response: oncostatin M signaling via MAPK in mouse cells	1.91E-05
Signal transduction: AKT signaling	3.08E-05
Immune response: oncostatin M signaling via MAPK in human cells	3.11E-05
Immune response: ETV3 effect on CSF1-promoted macrophage differentiation	3.11E-05
Development: thrombopoietin-regulated cell processes	4.46E-05
Cell adhesion: chemokines and adhesion	4.76E-05
Cell cycle: spindle assembly and chromosome separation	5.29E-05
Development: PIP3 signaling in cardiac myocytes	6.47E-05
Apoptosis and survival: BAD phosphorylation	9.78E-05
Development: growth hormone signaling via PI3K/AKT and MAPK cascades	9.78E-05
Apoptosis and survival: HTR1A signaling	0.000119062
Immune response: signaling pathway mediated by IL-6 and IL-1	0.000121599
Development: VEGF signaling via VEGFR2—generic cascades	0.000167581
Development: IGF-1 receptor signaling	0.000167581

APC, anaphase-promoting complex; BAD, Bcl-2-associated death promoter; IGF-1, insulin-like growth factor 1; IL, interleukin; MAPK, mitogen-activated protein kinase; TGF-β, transforming growth factor β.

DISCUSSION

The fetal heart is in a continuous state of remodeling, undergoing cardiomyocyte proliferation, enlargement, and differentiation. During the last third of gestation, these coordinated processes result in a marked increase in cardiac mass. We previously demonstrated that increased systolic load from ANG II infusion increases cardiac mass in fetal sheep, though specific effects on the cardiomyocyte were not investigated (5). In the current study, we demonstrate that increased fetal cardiac mass following ANG II–mediated increased cardiac load results primarily from hypertrophy of both mononucleated and binucleated cardiomyocytes. There also appears to be a contribution from cellular proliferation, as evidenced increased staining of the cell cycle activity marker, Ki-67. Because the ratio of mononucleated to binucleated cells did not significantly differ between groups despite an increase in LV cardiomyocyte cell cycle activity, ANG II appears to have little effect on the proportion of cells undergoing terminal differentiation. Although evidence for MAPK involvement was not found, microarray analysis from both ANG II– and losartan-exposed hearts identified several alternative pathways that may be involved in the fetal hearts response to altered load.

Normal physiologic fetal cardiac growth during the latter third of gestation primarily occurs through cellular proliferation and enlargement of myocytes as they undergo terminal differentiation (binucleation) with limited contribution from cellular hypertrophy (7). By contrast, pathologic cardiac adaptions to altered fetal cardiac load likely include both alterations

in proliferation and growth of mononucleated and binucleated cardiomyocytes. Pulmonary artery banding in fetal sheep results in increased cardiac mass, RV but not LV cardiomyocyte enlargement, and increased RV cardiomyocyte binucleation, suggestive of hyperplastic and hypertrophic growth (8). Increased fetal cardiac preload and afterload induced by daily intravascular plasma infusion increased in cardiac mass associated with cardiomyocyte hypertrophy, increased cell cycle activity, and increased percentage of binucleated cardiomyocytes (3). In this study, we found that ANG II was associated with increased cardiomyocyte area, and presumably volume. Additionally, increased Ki-67 staining in the LV suggests upregulation of cell cycle activity and thus proliferation. Evidence for more rapid progression of cardiomyocyte terminal differentiation was not seen. To study the effects of reduced systolic load on fetal cardiomyocyte development, O'Tierney *et al.* (6) utilized an 8-d infusion of enalaprilat, an angiotensin-converting enzyme inhibitor. Enalaprilat decreased arterial pressure by more than 20 mm Hg and significantly decreased heart weight-to-body weight ratio, suggesting attenuation of fetal heart growth. Cardiomyocyte size was not different between groups, though there was a significant decrease in LV and RV cardiomyocyte cell cycle activity, suggesting slowing of normal hyperplastic growth. Taken together, these studies emphasize the importance of cardiac load on cardiac growth.

Despite growing understanding of the pathologic changes that occur in the fetal heart with alterations in load, the molecular mechanisms regulating these changes remain poorly defined. Montgomery *et al.* (9) observed that RV loading from pulmonary artery banding altered expression of connexin isoforms involved in gap junction formation. In both aortic and pulmonary artery banded fetuses, levels of phosphorylated p38 were significantly increased as compared with controls, whereas no differences were identified in the levels of phosphorylated (activated) ERK or JNK (10). The role of p38 in the fetal heart has not been clearly defined, though evidence suggests that it promotes exit from the cell cycle, inducing myocyte differentiation and hypertrophy (11,12). In this study, we found that neither loading the heart with ANG II or unloading the heart with losartan resulted in significant changes in the levels of total or activated ERK, JNK, p38, or Akt. The absence of change in the expression of activated terminal kinases does not rule out their involvement in the observed responses, as we examined protein expression at single time point, well after the adaptive process has been initiated. The lack of change in the levels of activated MAPKs, through which ANG II is thought to directly signal cardiac hypertrophy, may also suggest that the effects of ANG II on the fetal heart result more from increased load of the heart rather than a direct effect mediated through cardiomyocyte ANG II receptors.

We utilized gene expression arrays performed on RNA isolated from a single area of the LV in ANG II- and losartan-infused fetal sheep and twin controls to explore molecular changes associated with manipulation of the fetal renin–angiotensin system. These studies show that losartan and ANG II infusion have generally opposing effects on the fetal cardiac transcriptome. The importance of the renin–ANG II axis on gene expression in the fetal heart is illustrated by the estimation that expression of more than 50% of the transcriptome was quantitatively altered by ANG II and/or losartan (see **Supplementary Table S1** online). Interestingly, blockade of the renin–angiotensin system in Wistar–Kyoto rats for 4 wk with candesartan, resulting in a significant decrease in systolic blood pressure (135 vs. 104 mm Hg), produced no significant changes in cardiac gene expression on a 9000 gene array (13). In contrast, we found AT_1 receptor blockade, which produced a significant decrease in fetal blood pressure, resulted in a large number of changes in gene expression. Our finding is consistent with the apparent dependence of load in regulating fetal cardiomyocyte proliferation and hypertrophy (6).

To further explore mechanisms contributing to load-related remodeling of the fetal heart, we utilized results from the gene expression arrays to perform biological pathway analysis. This approach allows for identification of potential biochemical and molecular processes in the fetal heart affected by manipulation of the renin–ANG II system. Our model holds a particular uniqueness in that studies in adult animals suggest that pathologic cardiac hypertrophy is accompanied by activation of "fetal cardiac genes" and that a similar transcriptional program regulates hypertrophic cardiac growth and controls early cardiac development. Whether fetal cardiac hypertrophy represents overactivity of transcriptional regulators of normal development or involves separate pathways is not known. Chief among the pathways identified as highly impacted by fetal renin–angiotensin system modulation are those involved in cytoskeletal remodeling, transcriptional regulation, and cell cycle activity (**Table 2**). An impact on skeletal remodeling pathways has been previously observed in the loaded or unloaded heart in several adult species, including flies and rodents (14–17). Murine cardiac transcriptome analysis following chronic ANG II infusion found the largest group of altered genes to be related to extracellular matrix, cell membrane, and nuclear pathways (18). Among the 25 top scoring pathways altered by renin–angiotensin system modulation were also a large number involving transforming growth factor β signaling and inflammatory pathways. Identification of transforming growth factor β pathways is not surprising given their known importance in the cardiac response to pressure overload and ANG II (19,20). There is growing evidence that inflammation plays a role in cardiac hypertrophy, and in particular cytokines activated downstream of nuclear factor kB (21). Along these lines, NFkB and the transcription factor AP-1 are activated by ANG II and in the postnatal heart contribute to ANG II–induced hypertrophy (22). The importance of the interleukin 6 pathway (item 5 on **Table 2**) in several different models of cardiac hypertrophy has also recently been highlighted (23,24). Taken together, these findings suggest that many of the molecular adaptations that take place in pathologic hypertrophy in the adult heart are present in response to increased pressure load in the fetal heart.

The ability to discern biological pathways regulating (i) cardiomyocyte hyperplasia from those of hypertrophy and

(ii) cardiac responses to mechanical stress from those of humoral factors would mark tremendous progress in understanding the adaptive response of the fetal heart to increased load. As yet, however, we are unable to identify such links. Isolated and cultured neonatal and fetal myocytes have been primarily used to study the regulation of cardiomyocyte proliferation. Both chemical and mechanical factors, including pressure load, ANG II, isoproterenol, cortisol, growth hormone, and insulin-like growth factor 1, have been shown to stimulate proliferation utilizing overlapping and complementary pathways (2,25–27). Signaling pathways associated with these factors involve Akt, phosphoinositol 3-kinase (PI3K), ERK, Ras, and gp130 (28,29). Our findings of significant changes in a number of signaling pathways involving these factors (e.g., Akt signaling, PIP3 signaling in cardiac myocytes, interleukin 6 signaling pathways, and insulin-like growth factor 1 receptor signaling; **Table 2**) supports the importance of these pathways in the adaptive changes that we observed in the fetal heart.

Our study has a number of limitations. We are unable to differentiate the routes of influence by which ANG II affects cardiomyocytes. More specifically, we cannot separate the direct effects of activation or blockade of cardiac AT_1 receptors from indirect effects on the heart by changes in pressure load. Our control animals, which were paired twins, were not surgically instrumented as were study animals, and thus not perfect controls. We also did not perform validation of specific gene changes by quantitative PCR. Such studies will be important as we move forward in understanding molecular regulation of physiologic and pathologic fetal heart growth. Furthermore, the microarray studies were performed on cardiac ventricular wall tissue homogenates and not isolated myocytes. The potential contribution of nonmyocyte tissue to the expression data is recognized. We also did not perform any histological evaluation of the cardiac tissue to address whether an inflammatory process was present and potentially contributing to the transcriptome and signaling pathway results. Lastly, gene expression and protein levels were assessed at only a single time point in the development of increased cardiac mass. Had measurements been performed at an earlier time point, a different profile of gene expression likely would be evident.

In summary, our studies indicate that *in vivo*, ANG II increases fetal LV mass primarily by induction of cardiomyocyte proliferation and hypertrophy. Despite a well-described role for MAPKs in regulating pathologic cardiac growth, no involvement of terminal MAPK proteins was identified at the time point measured. To our knowledge, this study represents the first to examine changes in the transcriptome of the fetal heart in response to pressure load in an animal with a similar developmental pattern to the human. The use of gene expression profiling to identify potential signaling pathways altered in response to pressure loading and unloading that may help delineate molecular mechanisms of adaptive growth of the fetal heart. These findings provide a foundation for future experiments in the underexplored area of fetal heart growth.

METHODS

Animals and Surgical Preparation

All procedures were performed within the regulations of the Animal Welfare Act and the National Institutes of Health (Bethesda, MD) *Guide for the Care and Use of Laboratory Animals* and approved by the University of Iowa Animal Care and Use Committee. Time-bred pregnant ewes of mixed Dorset-Suffolk breed were obtained from a local supplier and acclimated to the laboratory over several days.

Pregnant ewes at 125–126 d of gestation (term 145 d) with twin fetal pregnancies were used for the study (n = 15 ewes). Anesthesia was induced with 12 mg/kg of thiopental sodium (Pentothal Sodium, Abbott Laboratories) and maintained with a mixture of isoflurane (1–3%), oxygen (30%), and nitrous oxide. Under sterile conditions, the uterus was opened over the fetal hind limbs. Indwelling catheters (PE-90, inner diameter = 0.86 mm, outer diameter = 1.27 mm; Intramedic, Franklin Lakes, NJ) were placed into the right fetal femoral artery and vein, and a catheter for measurement of amniotic pressure was secured to the fetal skin. Control twin fetuses were not instrumented to avoid a second uterine incision and inadvertent manipulation of the first fetus that would increase the risk for loss of the surgical preparation. All incisions were closed in separate layers, and catheters were exteriorized through a subcutaneous tunnel and placed in a cloth pouch on the ewe's flank. Ampicillin sodium (2 g) (Wyeth Laboratories, Philadelphia, PA) was administered to the ewe prior to surgery, intra-amniotically at the completion of surgery and daily for 3 d. Pregnant ewes were returned to individual pens and allowed free access to food and water. Butorphanol (0.1 mg/kg i.v., Torbugesic; Fort Dodge Animal Health, Fort Dodge, IA) was given for 24 h postoperatively for analgesia. Animals were allowed 24-h recovery after surgical preparation before physiologic measurements were begun.

Experimental Protocols

To address the separate aims of the study, two sets of experiments were performed. To examine heart and cardiomyocyte growth in response to ANG II, the catheterized fetus received a continuous intravenous infusion of ANG II (50 ug /kg/min, 0.5 ml/h) using a battery operated Pegasus VARIO micro-piston pump (Instech Lab, Plymouth Meeting, PA). Physiological measurements were obtained prior to initiating the infusion, then daily for 5 d. Ewes were confined to stanchions during the recording periods, though afforded free access to food and water. Pressures were recorded with Transpac pressure transducers (Abbott, Abbott Park, IL) on a calibrated computerized system (AD Instruments, Colorado Springs, CO). Fetal arterial pressures were referenced to amniotic fluid pressure. Arterial pressure tracings were used to determine fetal heart rate. Fetal arterial blood samples were taken daily for blood gases and pH (Gem Premier 3000; Instrumentation Laboratory, Bedford, MA).

Tissue Collection, Cardiac Dissociation, and Cardiomyocyte Analysis

At the completion of the infusion, ewes were anesthetized, and the fetuses were exteriorized and administered heparin (5000 U i.v.) and saturated potassium chloride (10 ml i.v.) to arrest their hearts in diastole. Fetuses and excised hearts were weighed. Fetal hearts were then enzymatically dissociated on a Langendorff apparatus, and the cardiomyocytes fixed for morphometric analysis with the long-axis (length) and maximal cross-sectional diameter (width) dimensions of cardiomyocytes measured as previously described (3). Fixed myocytes were prepared in a wet mount with methylene blue, and selected for measurement according to a random, nonrepeating, and unbiased method using a counting frame. Myocytes were photographed at 40× on a light microscope (Zeiss Axiophot, Bellevue, WA), and photomicrographs analyzed using calibrated Optimas software (Optimas, Seattle, WA) and Image J software (National Institutes of Health). At least 50 cells of each type (mononucleated or binucleated) were measured per ventricle per fetus. Separately, cells were stained with hematoxylin and eosin, and at least 300 myocytes from each ventricle of each fetus were counted to determine the number of nuclei per cardiomyocyte.

Cell Cycle Activity

The anti–Ki-67 antibody MIB-1 (DAKO, Carpinteria, CA) was used to immunohistologically detect cell cycle activity in dissociated cardiomyocytes as described (3). No fewer than 500 mononucleated myocytes were counted per ventricle per fetus for cell cycle activity analysis. Ki-67–positive myocytes are expressed as a percent of total mononucleated cardiomyocytes.

Morphometry Data Analysis

Values are presented as means ± SEM. Statistical comparisons were performed by Student's unpaired, two-tailed *t*-test or ANOVA with Tukey's *post hoc* test if the *F* statistic was found to be significant. A value of $P < 0.05$ was considered significant.

The second series of studies investigated mechanisms regulating adaptive changes in the fetal heart in response to loading and unloading of the heart with ANG II and the AT_1 receptor antagonist, losartan, respectively. Catheterized fetuses received either an infusion of ANG II, as described above, or losartan (20 mg/kg est. fetal weight, i.v.) on a daily basis for 5 d with the twin serving as a control. Physiological measurements were obtained daily for 5 d, following which fetuses were euthanized as described above. Fetuses were weighed, and their hearts were removed. A portion of the left ventricular free wall, 1 cm below the atrioventricular groove, 0.5 cm in width, and extending to within 0.5 cm of the septum was quickly excised, weighed, frozen in liquid nitrogen, and stored at −80 °C. This tissue was used for RNA isolation and microarray analysis as described below. The remainder of the heart was dissected into anatomical components, weighed, and immediately frozen in liquid nitrogen. Ewes were killed by intravenous administration of pentobarbital sodium (Euthasol Solution; Virbac, Fort Worth, TX).

Quantitative Immunoblot

Immunoblots were performed to quantify protein expression (10). Primary antibodies were from Santa Cruz Biotechnology (Santa Cruz, CA) that were specific to total ERK1/2 (sc-93), phosphorylated ERK1/2 (sc-7383), total JNK1/2 (sc-1648), and phosphorylated JNK1/2 (sc-6254) and from Cell Signaling Technology (Beverly, MA) that were specific to Akt (9272), phosphorylated (Ser-473) Akt (9271), p38 (9212), and phospho-p38 (9211).

RNA Isolation and Microarray Assay

Frozen tissues were shipped to MOgene (St Louis, MO) on dry ice. High-quality RNA was isolated (RNA Integrity Number of 7.5–10 and 28S/18S ratio of 1.6–2.1) and confirmed with an Agilent Bioanalyzer at MOgene. Five hundred nanograms of total RNA was amplified using Agilent QuickAmp Labeling Kit (no dye; Agilent Technologies, Santa Clara, CA) and purified using Zymo Research (Irvine, CA) RNA Clean and Concentrator spin columns. Three micrograms of amplified RNA was Cy-labeled using the Kreatech ULS Labeling Kit, fragmented according to Agilent specifications and hybridized to the Agilent sheep gene expression microarray for 17 h at 65 °C and 10 rpm. Slides were scanned on an Agilent C scanner (20 bit) at 5 μm resolution. Sixteen microarray hybridizations were performed, each with samples from ANG II- or losartan-infused fetus ($n = 4$ for each) or a paired twin control ($n = 8$), using a mixed design on two slides with eight microarrays per slide. Microarray data were submitted to the NCBI Gene Expression Omnibus and can be accessed at http://www.ncbi.nlm.nih.gov/geo/query/acc.cgi?acc=GSE45463 (project accession no: GSE45463).

Microarray Quality Control

Hybridization scans were free of visual artifacts. Spike-in probe sets exhibited strong linear relationships between concentration and signal intensity for all 16 microarrays (each microarray $R^2 > 0.99$).

Microarray Gene Annotation

At the time of analysis, public annotations of gene identities for the sheep transcriptome were largely incomplete. Therefore, identities of sheep microarray oligonucleotide sequences lacking public annotation were assigned, where possible, based on interspecies homology (30) using *blastn* (31) on the NCBI 'nr' database accessed 1–4 December 2011. The accession of each top scoring hit was then cross-referenced for a match at Entrez Gene (32), and if none present, then at Entrez Nucleotide (33).

Microarray Analysis

Microarray analysis was performed using the open source R (R Development Core Team, University of Auckland, Auckland, NZ) and Bioconductor statistical environments (34). Preprocessing employed background correction using a saddle-point approximation to maximum likelihood (35) and quantile normalization using the "limma" package (36). *ComBat*, an empirical Bayes framework robust with small sample sizes, was used to minimize batch effects (37). Data filtering, partitioning around medoids, principal component analysis, and hierarchical clustering were performed in R. Significant differences among group means was assessed using ANOVA. The proportion of the transcriptome experiencing differential expression was estimated by the method of Storey (38). To account for multiple comparisons, the pFDR was calculated using the "qvalue" package (38).

Pathway Analysis

Enrichment of significantly affected genes among pathways was investigated using the MetaCore database within the GeneGo pathway analysis software (Thomas Reuters, Carlsbad, CA). MetaCore does not offer pathway analysis for sheep-specific pathways; therefore, human homologs were used for the analysis. MetaCore pathways with a probabilistic overrepresentation of statistically significant genes were determined using Fisher's exact test, controlling for a FDR of 0.05.

SUPPLEMENTARY MATERIAL

Supplementary material is linked to the online version of the paper at http://www.nature.com/pr

STATEMENT OF FINANCIAL SUPPORT

This work was supported by the National Institutes of Health (Bethesda, MD) grant DK097820 and University of Iowa Fraternal Order of Eagles Diabetes Research Center pilot grant (to A.W.N.) and National Institutes of Health HL080657 (to J.L.S.).

Disclosure: The authors declare no conflicts of interest.

REFERENCES

1. Barry SP, Davidson SM, Townsend PA. Molecular regulation of cardiac hypertrophy. Int J Biochem Cell Biol 2008;40:2023–39.
2. Thornburg K, Jonker S, O'Tierney P, et al. Regulation of the cardiomyocyte population in the developing heart. Prog Biophys Mol Biol 2011;106:289–99.
3. Jonker SS, Faber JJ, Anderson DF, Thornburg KL, Louey S, Giraud GD. Sequential growth of fetal sheep cardiac myocytes in response to simultaneous arterial and venous hypertension. Am J Physiol Regul Integr Comp Physiol 2007;292:R913–9.
4. Schlüter KD, Wenzel S. Angiotensin II: a hormone involved in and contributing to pro-hypertrophic cardiac networks and target of anti-hypertrophic cross-talks. Pharmacol Ther 2008;119:311–25.
5. Segar JL, Dalshaug GB, Bedell KA, Smith OM, Scholz TD. Angiotensin II in cardiac pressure-overload hypertrophy in fetal sheep. Am J Physiol Regul Integr Comp Physiol 2001;281:R2037–47.
6. O'Tierney PF, Anderson DF, Faber JJ, Louey S, Thornburg KL, Giraud GD. Reduced systolic pressure load decreases cell-cycle activity in the fetal sheep heart. Am J Physiol Regul Integr Comp Physiol 2010;299:R573–8.
7. Jonker SS, Zhang L, Louey S, Giraud GD, Thornburg KL, Faber JJ. Myocyte enlargement, differentiation, and proliferation kinetics in the fetal sheep heart. J Appl Physiol (1985) 2007;102:1130–42.
8. Barbera A, Giraud GD, Reller MD, Maylie J, Morton MJ, Thornburg KL. Right ventricular systolic pressure load alters myocyte maturation in fetal sheep. Am J Physiol Regul Integr Comp Physiol 2000;279:R1157–64.
9. Montgomery MO, Jiao Y, Phillips SJ, et al. Alterations in sheep fetal right ventricular tissue with induced hemodynamic pressure overload. Basic Res Cardiol 1998;93:192–200.

10. Olson AK, Protheroe KN, Scholz TD, Segar JL. The mitogen-activated protein kinases and Akt are developmentally regulated in the chronically anemic fetal sheep heart. J Soc Gynecol Investig 2006;13:157–65.
11. Braz JC, Bueno OF, Liang Q, et al. Targeted inhibition of p38 MAPK promotes hypertrophic cardiomyopathy through upregulation of calcineurin-NFAT signaling. J Clin Invest 2003;111:1475–86.
12. Liao P, Georgakopoulos D, Kovacs A, et al. The *in vivo* role of p38 MAP kinases in cardiac remodeling and restrictive cardiomyopathy. Proc Natl Acad Sci USA 2001;98:12283–8.
13. Kato N, Liang YQ, Ochiai Y, Birukawa N, Serizawa M, Jesmin S. Candesartan-induced gene expression in five organs of stroke-prone spontaneously hypertensive rats. Hypertens Res 2008;31:1963–75.
14. Brooks WW, Bing OH, Conrad CH, et al. Captopril modifies gene expression in hypertrophied and failing hearts of aged spontaneously hypertensive rats. Hypertension 1997;30:1362–8.
15. Jin H, Yang R, Awad TA, et al. Effects of early angiotensin-converting enzyme inhibition on cardiac gene expression after acute myocardial infarction. Circulation 2001;103:736–42.
16. Kang BY, Hu C, Ryu S, et al. Genomics of cardiac remodeling in angiotensin II-treated wild-type and LOX-1-deficient mice. Physiol Genomics 2010;42:42–54.
17. Montana ES, Littleton JT. Expression profiling of a hypercontraction-induced myopathy in Drosophila suggests a compensatory cytoskeletal remodeling response. J Biol Chem 2006;281:8100–9.
18. Hu C, Dandapat A, Sun L, et al. Modulation of angiotensin II-mediated hypertension and cardiac remodeling by lectin-like oxidized low-density lipoprotein receptor-1 deletion. Hypertension 2008;52:556–62.
19. Koitabashi N, Danner T, Zaiman AL, et al. Pivotal role of cardiomyocyte TGF-β signaling in the murine pathological response to sustained pressure overload. J Clin Invest 2011;121:2301–12.
20. Rosenkranz S. TGF-beta1 and angiotensin networking in cardiac remodeling. Cardiovasc Res 2004;63:423–32.
21. Smeets PJ, Teunissen BE, Planavila A, et al. Inflammatory pathways are activated during cardiomyocyte hypertrophy and attenuated by peroxisome proliferator-activated receptors PPARalpha and PPARdelta. J Biol Chem 2008;283:29109–18.
22. Valente AJ, Clark RA, Siddesha JM, Siebenlist U, Chandrasekar B. CIKS (Act1 or TRAF3IP2) mediates angiotensin-II-induced interleukin-18 expression, and Nox2-dependent cardiomyocyte hypertrophy. J Mol Cell Cardiol 2012;53:113–24.
23. del Vescovo CD, Cotecchia S, Diviani D. A-kinase-anchoring protein-Lbc anchors IκB kinase β to support interleukin-6-mediated cardiomyocyte hypertrophy. Mol Cell Biol 2013;33:14–27.
24. Papay RS, Shi T, Piascik MT, Naga Prasad SV, Perez DM. α_1A-adrenergic receptors regulate cardiac hypertrophy *in vivo* through interleukin-6 secretion. Mol Pharmacol 2013;83:939–48.
25. Bernardo BC, Weeks KL, Pretorius L, McMullen JR. Molecular distinction between physiological and pathological cardiac hypertrophy: experimental findings and therapeutic strategies. Pharmacol Ther 2010;128:191–227.
26. Brüel A, Christoffersen TE, Nyengaard JR. Growth hormone increases the proliferation of existing cardiac myocytes and the total number of cardiac myocytes in the rat heart. Cardiovasc Res 2007;76:400–8.
27. Tseng YT, Yano N, Rojan A, et al. Ontogeny of phosphoinositide 3-kinase signaling in developing heart: effect of acute beta-adrenergic stimulation. Am J Physiol Heart Circ Physiol 2005;289:H1834–42.
28. MacLellan WR, Schneider MD. Genetic dissection of cardiac growth control pathways. Annu Rev Physiol 2000;62:289–319.
29. Sundgren NC, Giraud GD, Schultz JM, Lasarev MR, Stork PJ, Thornburg KL. Extracellular signal-regulated kinase and phosphoinositol-3 kinase mediate IGF-1 induced proliferation of fetal sheep cardiomyocytes. Am J Physiol Regul Integr Comp Physiol 2003;285:R1481–9.
30. Goyal R, Longo LD. Gene expression in sheep carotid arteries: major changes with maturational development. Pediatr Res 2012;72:137–46.
31. Altschul SF, Gish W, Miller W, Myers EW, Lipman DJ. Basic local alignment search tool. J Mol Biol 1990;215:403–10.
32. Maglott D, Ostell J, Pruitt KD, Tatusova T. Entrez Gene: gene-centered information at NCBI. Nucleic Acids Res 2005;33(Database issue):D54–8.
33. Wheeler DL, Barrett T, Benson DA, et al. Database resources of the National Center for Biotechnology Information. Nucleic Acids Res 2007;35(Database issue):D5–12.
34. Gentleman RC, Carey VJ, Bates DM, et al. Bioconductor: open software development for computational biology and bioinformatics. Genome Biol 2004;5:R80.
35. Silver JD, Ritchie ME, Smyth GK. Microarray background correction: maximum likelihood estimation for the normal-exponential convolution. Biostatistics 2009;10:352–63.
36. Smyth GK. Limma: linear models for microarray data. In: Gentleman R, Carey V, Dudoit S, Irizarry R, Huber W, eds. Bioinformatics and Computational Biology Solutions Using R and Bioconductor. New York, NY: Springer, 2005:397–420.
37. Johnson WE, Li C, Rabinovic A. Adjusting batch effects in microarray expression data using empirical Bayes methods. Biostatistics 2007;8:118–27.
38. Storey JD. A direct approach to false discovery rates. J R Stat Soc 2002;64:479–98.